

Oscillations of Solitonic Galactic Cores in Ultralight Dark Matter

L. Salasnich^{1,2} and A. Yakimenko^{1,3}

¹*Dipartimento di Fisica e Astronomia “Galileo Galilei”, Università di Padova,
and INFN, Sezione di Padova, Via Marzolo 8, 35131 Padova, Italy*

²*Istituto Nazionale di Ottica (INO) del Consiglio Nazionale delle Ricerche (CNR),
Via Nello Carrara 1, 50019 Sesto Fiorentino, Italy*

³*Department of Physics, Taras Shevchenko National University of Kyiv,
64/13, Volodymyrska Street, Kyiv 01601, Ukraine*

A remarkable feature of dark matter consisting of ultralight bosonic particles is the emergence of superfluid Bose-Einstein condensate structures on galactic scales. We investigate the oscillations of the solitonic dark matter structure in the central galactic region by numerically solving the Bogoliubov-de Gennes problem, accounting for perturbations in the gravitational potential and local self-interactions. Our findings reveal that the central solitonic core, formed by the balance of gravitational attraction, quantum pressure, and repulsive interactions, exhibits significant oscillatory behaviour. These oscillations, characterized by distinct eigenmodes, provide insights into the dynamical properties of solitonic dark matter structures and their observational implications and contributions to galactic structure formation and evolution.

I. INTRODUCTION

The physical nature of dark matter (DM) remains one of the most intriguing unresolved mysteries in modern physics. Among the various candidates for dark matter particles, ultra-light bosons, characterized by cosmic-scale Compton wavelengths, attract increasingly significant attention [1–5]. A key prediction of the ultralight dark matter (ULDM) theory is the emergence of a Bose–Einstein condensate (BEC) on galactic scales. The soliton-like BEC core in the central region of a galaxy represents a striking manifestation of quantum phenomena on cosmic scales.

In an ULDM halo, a central solitonic core coexists with standard cold dark matter density profile in the outer region. While a pure BEC soliton is typically stationary, recent studies [6] have shown that the central density of an isolated DM halo undergoes substantial time-dependent oscillations, deviating from strict soliton behavior. These oscillations in the perturbed solitonic core, observed in some ultrafaint dwarf galaxies, can lead to star cluster heating and a gradual increase in cluster size over time [7, 8]. In addition to internal oscillations, solitonic cores in ultralight dark matter halos can undergo a confined random walk due to continuous self-interference, impacting external gravity field related to the dynamics of satellite galaxies [9]. Consequently, the stability and dynamics of perturbed solitonic cores have been the subject of numerous theoretical investigations [10–30].

In particular, Refs. [10–12] examine the dynamics of the Schrödinger-Poisson (SP) system system in the absence of local self-interaction. This framework describes Fuzzy Dark Matter (FDM), a model of ultralight bosonic particles that form quantum states on galactic scales, exhibiting wave-like behavior. These studies numerically determined the eigenstates of the SP system using an averaged gravitational potential, assumed to be constant in time. As highlighted in Ref. [10], modeling the FDM halo as a superposition of energy eigenstates within a fixed

potential is a reasonable first approximation. However, the gravitational potential itself fluctuates over time, necessitating a self-consistent analysis of its perturbations. This rigorous approach is technically challenging due to the nonlocal nature of the gravitational potential. Since the gravitational potential perturbation is of the same order of magnitude as the density perturbation, solving the Bogoliubov-de Gennes (BdG) problem represents the next essential step in understanding solitonic BEC core perturbations. The BdG framework allows the systematic study of stability and collective modes by analyzing small perturbations around stationary states, crucial for understanding the dynamics of these quantum structures. Recent work [18] employed a perturbative method to examine the radial oscillatory dynamics of solitonic cores in fuzzy dark matter, revealing universal features across interaction regimes. Although radial analysis provides valuable insights, a comprehensive investigation of normal modes remains largely unexplored. Work [19] studied perturbations in a hybrid model which account both a coherent condensate state and an incoherent particlelike state. It was found in Ref. [13] that solitons, driven by repulsive self-interactions within extended halos of scalar-field dark matter, form rapidly and can constitute a significant portion of the total mass, with their formation and growth dependent on the system’s size and halo density profile. In addition to analysis of the eigenmodes with stationary potential in this work, an impact of different modes on the potential perturbation has been investigated. In a recent study [20] breathing and anisotropic modes have been investigated through numerical solutions of the GPP equations and variational methods.

In this work, we derive and numerically solve the complete BdG equations to analyze perturbations of the BEC solitonic core, accounting for gravitational potential fluctuations. Furthermore, we investigate the influence of local self-interactions, arising from repulsive bosonic interactions, on the excitations of the stationary solitonic state.

The paper is organized as follows. Section II presents the basic equations that govern the dynamics of self-gravitating BECs. In Section III, we recall the general properties of stationary solitonic cores. In Section IV, we introduce the BdG equations and describe the numerical methods used to solve them. Section V focuses on the breathing modes of the solitonic core. Finally, Section VI summarizes our findings and outlines potential directions for future research.

II. BASIC EQUATIONS

At zero temperature, the dynamics of a self-gravitating BEC of weakly interacting bosons in the mean-field approximation is described by the Gross-Pitaevskii-Poisson (GPP) equations. In dimensionless units, these equations take the form:

$$i\frac{\partial\Psi}{\partial t} = \left(-\frac{1}{2}\nabla^2 + \Phi + \gamma N_*|\Psi|^2\right)\Psi, \quad (1)$$

$$\nabla^2\Phi = N_*|\Psi|^2, \quad (2)$$

where $\Psi(\mathbf{r}, t)$ is the complex wave function of the condensate, normalized to unity:

$$\int |\Psi(\mathbf{r}, t)|^2 d\mathbf{r} = 1, \quad (3)$$

with $\mathbf{r} = (x, y, z)$ denoting spatial coordinates and t representing time. The Gross-Pitaevskii equation (1) describes evolution of the condensate with a nonlinearity arising from local interactions, while the gravitational potential $\Phi(\mathbf{r}, t)$, determined by the Poisson equation (2), introduces a nonlocal nonlinear interaction. Coefficient γ takes the value $+1$ for repulsive interparticle interaction, -1 for attractive interparticle interaction.

To obtain dimensional quantities the following relations can be used $\mathbf{r}_{\text{ph}} = \mathbf{r}L_*$, $t_{\text{ph}} = t/\Omega_*$, $\Phi_{\text{ph}} = \Phi\phi_*$, $\Psi_{\text{ph}} = \Psi\psi_*$, $E_{\text{ph}} = E\epsilon_*$, where $L_* = \lambda_C(m_{\text{Pl}}/m)\sqrt{\lambda/8\pi}$, $\Omega_* = c\lambda_C/L_*^2$, $\phi_* = (c\lambda_C/L_*)^2$, $\psi_* = mc^2/\left((\lambda/8\pi)(m_{\text{Pl}}/m)^2\sqrt{4\pi GM\hbar}\right)$, $\epsilon_* = \hbar^2(8\pi/\lambda)^{3/2}/(4\pi m_{\text{Pl}}\lambda_C^2)$, $m_{\text{Pl}} = \sqrt{\hbar c/G}$ is the Planck mass, $\lambda/8\pi = a_s/\lambda_C$ is the self-interaction constant with a_s being the s -wave scattering length, $\lambda_C = \hbar/mc$ is the Compton wavelength of the bosons and M is the total BEC cloud mass. The normalized number of particles in dimensionless units is given as follows:

$$N_* = 4\pi\frac{M}{m_{\text{Pl}}}\sqrt{\frac{\lambda}{8\pi}}. \quad (4)$$

where M is the mass of the solitonic core.

The total energy associated with the GPP system of equations can be written as

$$E = \Theta + U + W, \quad (5)$$

where, in the dimensionless units, the kinetic energy is

$$\Theta = \frac{1}{2}\int |\nabla\Psi|^2 d\mathbf{r}, \quad (6)$$

the internal energy

$$U = \frac{\gamma N_*}{2}\int |\Psi|^4 d\mathbf{r}, \quad (7)$$

and the gravitational potential energy of interaction is given by

$$W = \frac{1}{2}\int |\Psi|^2\Phi d\mathbf{r}. \quad (8)$$

In this work, we investigate the excitations of the solitonic core across a wide range of the dimensionless parameter N_* , as defined in Eq. (4), considering typical ultralight bosonic particle masses on the order of $m \sim 10^{-22}$ eV. These masses are consistent with the observed large-scale matter distribution [31–33], where quantum mechanical effects emerge on galactic scales. However, models with such light bosonic dark matter particles without local self-interaction have been shown to conflict with Lyman- α forest observations [34]. This inconsistency can be resolved if ULDM features non-negligible self-interactions. Consequently, we focus on the case of repulsive interparticle interactions ($\gamma = +1$) in this study.

Before proceeding to the study of excitations of the solitonic core, let us consider general properties of stationary self-gravitating BEC solitons.

III. STATIONARY SOLITONIC CORE

As a result of the balance between gravitational attraction, quantum pressure, and repulsive bosonic interparticle interaction, the system of equations (1) and (2) allows the existence of stationary solutions with the wave function

$$\Psi(\mathbf{r}, t) = \psi_0(r)e^{-i\mu t}, \quad (9)$$

where μ is the chemical potential and $\psi_0(r)$ is the radial profile of the wave function.

A. Numerical solitonic solutions

The stationary equation for the dimensionless ground state wave function $\psi_0(r)$ of the bosons in the BEC state is as follows:

$$\hat{\mathcal{H}}_l\psi_0(r) = 0, \quad (10)$$

where

$$\hat{\mathcal{H}}_l = -\mu - \frac{1}{2}\Delta_r^{(l)} + \gamma N_*\psi_0^2(r) + \Phi_0(r) \quad (11)$$

$$\Delta_r^{(l)} = \frac{d^2}{dr^2} + \frac{2}{r} \frac{d}{dr} - \frac{l(l+1)}{r^2}, \quad (12)$$

the gravitational potential for the spherically-symmetric solution is given as follows:

$$\Phi_0(r) = \Phi_0(0) - N_* \int_0^r \xi \psi_0^2(\xi) \left[1 - \frac{\xi}{r} \right] d\xi, \quad (13)$$

where

$$\Phi_0(0) = -N_* \int_0^{+\infty} \xi \psi_0^2(\xi) d\xi. \quad (14)$$

The normalization condition in dimensionless units is as follows:

$$4\pi \int_0^\infty \psi_0^2(\xi) \xi^2 d\xi = 1. \quad (15)$$

We solve numerically the set of Eq. (11), (13) of nonlinear integrodifferential equations using the stabilized relaxation procedure similar to that employed in Refs. [26, 35]

The typical example of numerically obtained ground-state solution is presented in Fig. 1 for $N_* = 100$, corresponding to a chemical potential $\mu = -2.2172$. The gray-scaled density plot shows the condensate density distribution, $|\psi_0|^2$, at $z = 0$ plane, in dimensionless units. The radial profile of the wave function, $\psi_0(r)$, is depicted by the solid blue line, while the red dashed line represents the radial profile of the normalized gravitational potential, $\Phi_0(r)/N_*$, generated by the self-gravitating solitonic core. Note that at large distances, the gravitational potential exhibits Coulomb-like asymptotics, whereas in the central region, it is well approximated by a harmonic oscillator potential.

Figure 2 presents stationary solitonic solutions of Eq. (10) with the norm determined by Eq. (15) for various values of parameter N_* . Figure 2 (a) shows the effective radius, r_{eff} , defined by

$$r_{\text{eff}}^2 = 4\pi \int_0^\infty \xi^4 \psi_0^2(\xi) d\xi. \quad (16)$$

The inset in Fig. 2 (a) depicts the corresponding radial profiles of the condensate density. Figure 2 (b) displays the chemical potential of the stationary state as a function of N_* . We further compare our numerically obtained stationary solitonic solutions with analytical estimates derived using the TF approximation.

B. Thomas-Fermi approximation

The influence of the local nonlinear term, corresponding to the repulsive self-interaction in the Gross-Pitaevskii equation, becomes increasingly significant with the growth of the dimensionless parameter N_* , as defined by Eq. (4). In Thomas-Fermi (TF) approximation neglecting the contribution of the quantum pressure

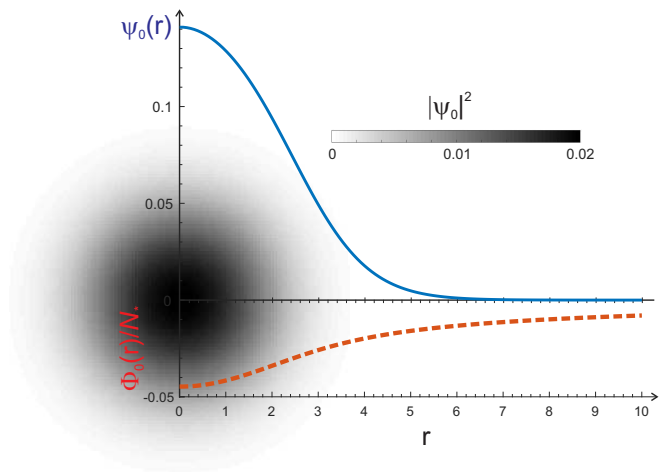


FIG. 1. Numerical stationary ground-state solution in dimensionless units for $N_* = 100$. The figure illustrates the radial profile of the condensate wave function $\psi_0(r)$ (solid blue line) and the normalized potential $\Phi_0(r)/N_*$ (dashed red line). The condensate density $|\psi_0|^2$ at $z = 0$ plane is represented in the grey-scale density plot.

in the equation of hydrostatic equilibrium [1] it is easy to obtain the normalized condensate density:

$$|\psi_{\text{TF}}(r)|^2 = \frac{1}{4\pi^2} \begin{cases} \frac{\sin r}{r}, & 0 \leq r \leq \pi \\ 0, & r > \pi \end{cases} \quad (17)$$

and corresponding gravitational potential:

$$\Phi_{\text{TF}}(r) = -\frac{N_*}{4\pi^2} \begin{cases} 1 + \frac{\sin r}{r}, & 0 \leq r \leq \pi \\ \frac{\pi}{r}, & r > \pi. \end{cases} \quad (18)$$

The TF radius of the solitonic core $R_{\text{TF}} = \pi$, effective radius of the solitonic core: $r_{\text{eff}} = \sqrt{\pi^2 - 6} \approx 1.967$, $\psi_{\text{TF}}(0) = \frac{1}{2\pi}$, $\Phi_{\text{TF}}(0) = -\frac{N_*}{2\pi^2}$. The chemical potential in TF approximation is: $\mu_{\text{TF}} = -\frac{N_*}{4\pi^2}$.

The inset in Fig. 2 (a) and Fig. 2 (b) compare the density distribution $|\psi_{\text{TF}}|^2$ and chemical potential μ_{TF} as a function of N_* with the corresponding numerical results. As N_* increases, the numerically found radial profiles exhibit a smooth convergence toward the TF limit. The effective radius of the solitonic core, calculated from the numerical solution of the stationary Gross-Pitaevskii equation, approaches the value of r_{eff} obtained in the TF approximation [indicated by the dashed blue line in Fig. 2(a)] in the limit $N_* \gg 1$.

IV. BOGOLIUBOV-DE GENNES EQUATIONS

The important information on dynamics of the solitons can be obtained from the analysis of small perturbations of the stationary states. The basic idea of such a linear stability analysis is to represent a linear perturbation as a superposition of the modes with different angular symmetries.

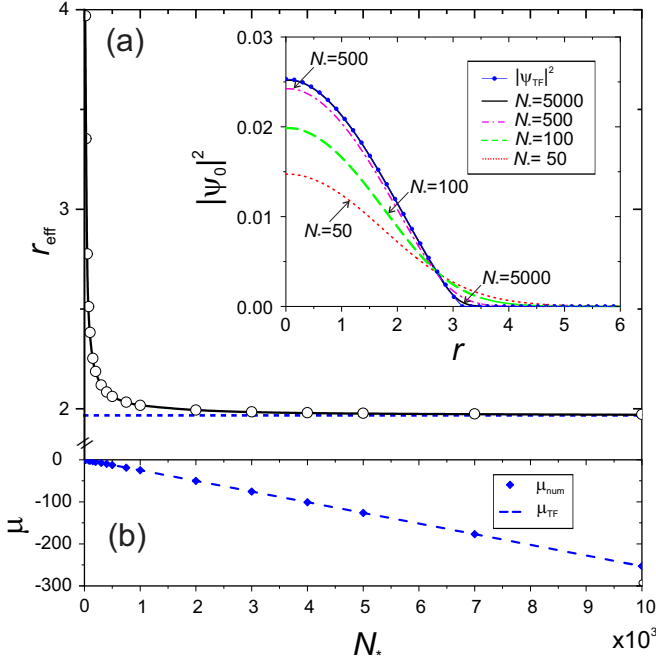


FIG. 2. (a) Effective radius vs normalized number of bosonic particles N_* . The inset illustrates the radial profiles of the condensate density $|\psi_0|^2$ for different N_* . (b) chemical potential μ vs N_* . Shown are the results of numerical simulations (blue diamonds) and Thomas Fermi approximation (dashed blue line).

Since the perturbation is assumed to be small, the dynamics of each linear mode can be studied independently. Presenting the nonstationary solution in the vicinity of the stationary state as follows,

$$\Psi(\mathbf{r}, t) = [\psi_0(r) + \delta\psi(\mathbf{r}, t)] e^{-i\mu t}, \quad \Phi(\mathbf{r}, t) = \Phi_0(r) + \delta\Phi(\mathbf{r}, t) \quad (19)$$

$$\delta\psi(\mathbf{r}, t) = u_l(r) Y_{lm_z}(\theta, \varphi) e^{-i\omega t} + v_l^*(r) Y_{lm_z}^*(\theta, \varphi) e^{i\omega^* t} \quad (20)$$

By inserting Eqs. (19) and (20) into Eqs. (1) and (2), and linearizing with respect to small perturbations, we obtain the BdG equations:

$$\hat{\mathcal{H}}_l u_l + \gamma N_* \psi_0^2 v_l + \psi_0 \hat{D} * (\psi_0^* u_l + \psi_0 v_l) = \omega u_l, \quad (21)$$

$$\hat{\mathcal{H}}_l v_l + \gamma N_* \psi_0^2 u_l + \psi_0 \hat{D} * (\psi_0^* u_l + \psi_0 v_l) = -\omega v_l, \quad (22)$$

where $y(r) = \hat{D} * f(r)$ denotes the solutions of the radial equation:

$$\Delta_r^{(l)} y(r) = f(r). \quad (23)$$

Further, we focus on the ground state of the spherically symmetric wave function of the solitonic core, $\psi_0(r)$. This wave function is real and satisfies the stationary equation (10).

Thus the BdG equations can be rewritten in the following form:

$$\hat{\mathcal{H}}_l u_l + \hat{\chi}_l \{\psi_0(u_l + v_l)\} + \gamma N_* \psi_0^2 (u_l + v_l) = \omega u_l, \quad (24)$$

$$\hat{\mathcal{H}}_l v_l + \hat{\chi}_l \{\psi_0(u_l + v_l)\} + \gamma N_* \psi_0^2 (u_l + v_l) = -\omega v_l, \quad (25)$$

where

$$\hat{\chi}_l \{f\} = -N_* \psi_0(r) \int_0^{+\infty} G_l(r, \xi) \psi_0(\xi) f(\xi) d\xi, \quad (26)$$

and

$$G_l(r, \xi) = \frac{\xi}{2l+1} \begin{cases} [\xi/r]^{l+1}, & 0 \leq \xi \leq r \\ [r/\xi]^l, & r \leq \xi < \infty \end{cases} \quad (27)$$

Note that $\hat{\chi}_{l=0} \{\psi_0\} = \psi_0(r) \Phi_0(r)$, as it must be.

The matrix form of the BdG eigenvalue problem in dimensionless units is as follows:

$$\begin{pmatrix} \mathcal{B}_{11}^{(l)} & \mathcal{B}_{12}^{(l)} \\ \mathcal{B}_{21}^{(l)} & \mathcal{B}_{22}^{(l)} \end{pmatrix} \begin{pmatrix} u_l \\ v_l \end{pmatrix} = \omega_{\nu l} \begin{pmatrix} u_l \\ v_l \end{pmatrix}, \quad (28)$$

where $\mathcal{B}_{11}^{(l)} = \hat{\mathcal{H}}_l + \mathcal{B}_{12}^{(l)}$, $\mathcal{B}_{12}^{(l)} = \gamma N_* \psi_0^2 + \hat{\chi}_l$, $\mathcal{B}_{21}^{(l)} = -\mathcal{B}_{12}^{(l)}$, $\mathcal{B}_{22}^{(l)} = -\mathcal{B}_{11}^{(l)}$.

The boundary conditions for eigenfunctions for $l \neq 0$ and for $l = 0$ at the center of the solitonic core are as follows:

$$u_l(0) = v_l(0) = 0, \quad \left. \frac{du_l}{dr} \right|_{r=0} = \left. \frac{dv_l}{dr} \right|_{r=0} = 0, \quad (29)$$

and at infinity for all l :

$$\lim_{r \rightarrow \infty} u_l(r) = \lim_{r \rightarrow \infty} v_l(r) = 0. \quad (30)$$

The dimensionless radial eigenfunctions $u_l(r)$ and $v_l(r)$ are rescaled to satisfy the normalization condition:

$$\int_0^{+\infty} (|u_l(\xi)|^2 - |v_l(\xi)|^2) \xi^2 d\xi = \frac{1}{\psi_*^2 L_*^3}. \quad (31)$$

The BdG eigenvalue problem (28) with an integrodifferential operator can be represented in finite-difference form with zero boundary conditions $u_l(r_{\text{max}}) = 0$, $v_l(r_{\text{max}}) = 0$ at the endpoint of the radial grid $r = r_{\text{max}}$. We have solved the resulting linear algebra eigenvalue problem numerically. It turns out that this approach gives an accurate description for the lower-order states for large enough N_* , when the eigenfunctions are well localized. However, this method is not able to accurately represent the increasingly large-scale eigenfunctions at higher ν and l values since the spectrum becomes sensitive to the boundary conditions at r_{max} , as was pointed out in Ref. [12]. Thus, as the quantum numbers ν and l increase in BdG equations, numerical solutions require a more sophisticated approach.

In the present work, we have developed a method for the solution of the complete BdG problem with the integrodifferential operator which is valid for arbitrary quantum numbers ν , l including highly-excited states with $\nu \gg 1$ or $l \gg 1$. Since BdG set of equations is linear, we suggest representing the radial profiles $u_l(r)$ and $v_l(r)$ as the following linear superposition:

$$\begin{pmatrix} u_l(r) \\ v_l(r) \end{pmatrix} = \sum_{\nu=0}^{\infty} \begin{pmatrix} U_{\nu}^{(l)} \\ V_{\nu}^{(l)} \end{pmatrix} R_{\nu l}(r), \quad (32)$$

where $U_{\nu}^{(l)}$ and $V_{\nu}^{(l)}$ are constants and functions $R_{\nu l}(r)$, form a complete orthonormal set of functions

$$\int_0^{+\infty} R_{\alpha l}(r) R_{\nu l}(r) r^2 dr = \delta_{\alpha\nu}. \quad (33)$$

Various orthogonal bases can be used to solve the linear BdG problem. In the present work, we have used two different basis functions: (i) a basis of the hydrogen-like atom (H-like basis) and (ii) a basis of the 3D spherically symmetric quantum harmonic oscillator (QHO basis). Both solutions being converging, give the same results for the eigenstates but exhibit different speeds of convergence for different quantum numbers ν and l . In both cases, we choose the radial basis functions, $R_{\nu l}(r)$, in *analytic form*, which allows us to accurately describe the spectrum ω and eigenfunctions $u_l(r)$, $v_l(r)$ for arbitrary quantum numbers ν and l . Each radial function satisfies the following ordinary differential equation:

$$-\frac{1}{2}\Delta_r^{(l)} R_{\nu l}(r) + \Phi_B(r) R_{\nu l}(r) = E_{\nu l} R_{\nu l}(r), \quad (34)$$

where the trapping potential $\Phi_B(r)$ for the radial basis functions is chosen to accurately describe details of the self-induced gravitational potential $\Phi_0(r)$ either in the central region (for a basis of the 3D spherically symmetric quantum harmonic oscillator) or asymptotic behaviour for a large distance from the BEC core centre (H-like basis). The energy $E_{\nu l}$ in Eq. (34) does not depend on the quantum number m_z due to the spherical symmetry of the potential $\Phi_B(r)$.

To obtain a numerical solution to the BdG problem we need to calculate the set of coefficients in expansion (32), which form the vectors $\mathbf{U}^{(l)} = \{U_0^{(l)}, U_1^{(l)}, \dots, U_{\nu_{\max}}^{(l)}\}$, $\mathbf{V}^{(l)} = \{V_0^{(l)}, V_1^{(l)}, \dots, V_{\nu_{\max}}^{(l)}\}$, where ν_{\max} is chosen to guarantee a desirable accuracy in converging sum (32). A detailed analysis of basis convergence and the appropriate selection of the number of basis functions, both for the QHO and the H-like basis, is presented in the Appendix.

Let us insert expansion (32) in Eqs. (24),(25), accounting on Eq. (34) and orthogonality condition (33), which yields the following linear algebraic eigenvalue problem:

$$\sum_{\nu=0}^{\nu_{\max}} \left[\mathcal{H}_{\alpha\nu}^{(l)} U_{\nu}^{(l)} + \mathcal{K}_{\alpha\nu}^{(l)} (U_{\nu}^{(l)} + V_{\nu}^{(l)}) \right] = \omega U_{\alpha}^{(l)} \quad (35)$$

$$\sum_{\nu=0}^{\nu_{\max}} \left[\mathcal{H}_{\alpha\nu}^{(l)} V_{\nu}^{(l)} + \mathcal{K}_{\alpha\nu}^{(l)} (U_{\nu}^{(l)} + V_{\nu}^{(l)}) \right] = -\omega V_{\alpha}^{(l)} \quad (36)$$

where $\mathcal{H}_{\alpha\nu}^{(l)}$ is the matrix element of operator $\hat{\mathcal{H}}^{(l)}$ defined in Eq. (11):

$$\begin{aligned} \mathcal{H}_{\alpha\nu}^{(l)} &= \int_0^{+\infty} r^2 R_{\alpha l}(r) \hat{\mathcal{H}}_l R_{\nu l}(r) dr \\ &= (-\mu + E_{\alpha l}) \delta_{\alpha\nu} + \mathcal{F}_{\alpha\nu}^{(l)} + \mathcal{P}_{\alpha\nu}^{(l)}, \end{aligned} \quad (37)$$

where $\delta_{\alpha\nu}$ is the Kronecker delta and

$$\mathcal{F}_{\alpha\nu}^{(l)} = \int_0^{+\infty} [\Phi_0(r) - \Phi_B(r)] R_{\alpha l}(r) R_{\nu l}(r) r^2 dr, \quad (38)$$

$$\mathcal{P}_{\alpha\nu}^{(l)} = \gamma N_* \int_0^{+\infty} \psi_0^2(r) R_{\alpha l}(r) R_{\nu l}(r) r^2 dr. \quad (39)$$

The matrix $\hat{\mathcal{K}}^{(l)}$ in Eqs. (35), (36) is defined as follows:

$$\mathcal{K}_{\alpha\nu}^{(l)} = \mathcal{P}_{\alpha\nu}^{(l)} - \mathcal{Q}_{\alpha\nu}^{(l)}, \quad (40)$$

where

$$\mathcal{Q}_{\alpha\nu}^{(l)} = N_* \int_0^{+\infty} \int_0^{+\infty} q_{\alpha\nu}^{(l)}(r, \xi) r^2 dr d\xi, \quad (41)$$

$$q_{\alpha\nu}^{(l)}(r, \xi) = \psi_0(r) \psi_0(\xi) G_l(r, \xi) R_{\alpha l}(r) R_{\nu l}(\xi). \quad (42)$$

Let us rewrite BdG equations using the symmetric and antisymmetric superposition of the eigenvectors: $\mathbf{S} = \mathbf{U}^{(l)} + \mathbf{V}^{(l)}$ and $\mathbf{A} = \mathbf{U}^{(l)} - \mathbf{V}^{(l)}$ as follows: $\hat{B}_- \mathbf{A} = \omega \mathbf{S}$ and $\hat{B}_+ \mathbf{S} = \omega \mathbf{A}$, where $(\hat{B}_-)_{\alpha\nu} = \mathcal{H}_{\alpha\nu}^{(l)}$ and $(\hat{B}_+)_{\alpha\nu} = \mathcal{H}_{\alpha\nu}^{(l)} + 2\mathcal{K}_{\alpha\nu}^{(l)}$. Finally we obtain two decoupled linear eigensystems for \mathbf{A} and \mathbf{S} :

$$\hat{B}_+ \hat{B}_- \mathbf{A} = \omega^2 \mathbf{A}, \quad (43)$$

$$\hat{B}_- \hat{B}_+ \mathbf{S} = \omega^2 \mathbf{S}. \quad (44)$$

These eigensystems have been solved numerically for various values of the parameter N_* .

Numerical results for the eigenvalues are presented in Fig. 3 for $N_* = 100$. The inset of Fig.3 displays typical eigenfunction profiles $u_l(r)$ and $v_l(r)$ for $l = 0$ and $l = 2$ and illustrating different numbers of nodes in the radial profiles. The corresponding eigenvalues are denoted by capital-letter symbols in Fig. 3. Arbitrary units are used for the eigenfunctions to avoid the very small values imposed by the normalization condition (31).

All eigenfrequencies of the solitonic ground-state perturbations are real, confirming the well-established stability of ground-state solitonic configurations under repulsive self-interaction (see, e.g., [1, 36]). The eigenfrequencies of highly excited states with $\nu \gg 1$ and $l \gg 1$ are well approximated by $\omega_{\nu l} \approx -\mu + E_{\nu l}$, where $E_{\nu l}$ represents the energy of a hydrogen-like system:

$$E_{\nu l} = -\frac{Z^2}{2(\nu + l + 1)^2}. \quad (45)$$

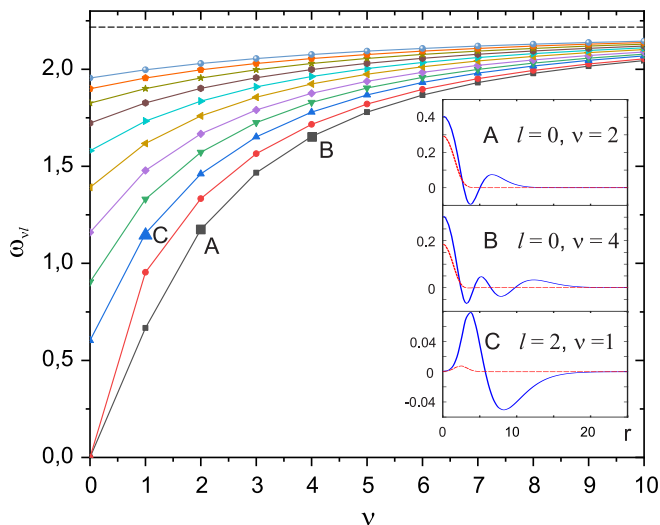


FIG. 3. Eigenfrequencies $\omega_{\nu l}$ for $l \in [0, 10]$, calculated numerically from the Bogoliubov-de Gennes equations for $N_* = 100$. The inset shows examples of the eigenfunctions (in arbitrary units) for different values of quantum numbers ν and l .

In the limit $\nu \gg 1$ and $l \gg 1$, $\omega_{\nu l} \rightarrow -\mu$, as illustrated in Fig. 3. The black dashed line in the figure indicates the asymptotic value $-\mu$.

The lowest-energy solution is given by the wave functions $u_{00}(r) = \psi_0(r)$, $v_{00}(r) = -\psi_0(r)$, with the eigenvalue $\omega_{00} = 0$. Notably, the dipole-like $l = 1$ node-less mode $\nu = 0$ also corresponds to the zeroth frequency. However, this mode does not represent an excitation of the ground state but rather produces a center-of-mass motion, and we do not consider this type of perturbation in the present work.

The lowest non-zero-frequency mode corresponds to the eigenstate with $l = 0$ and a single node ($\nu = 1$). This mode represents periodic breathing, characterized by low-frequency, radially symmetric oscillations of the solitonic core. We further investigate these oscillations in detail and compare our numerical results with predictions from a simple variational approach.

V. BREATHING EXCITATIONS OF THE SOLITONIC CORE

In this section, we study the compressible mode $\nu = 1$, $l = 0$, which represents low-frequency oscillations of the solitonic core. To gain a deeper understanding of these radially symmetric oscillations, we compare our numerical results with analytical predictions obtained by variational method.

Here we use a standard variational approach (see, e.g., [1, 37]) with a normalized Gaussian trial function in dimensionless form:

$$\Psi(\mathbf{r}, t) = \frac{1}{\sqrt{\pi^{3/2} R^3(t)}} e^{-\frac{r^2}{2R^2(t)} + i\beta(t)r^2}, \quad (46)$$

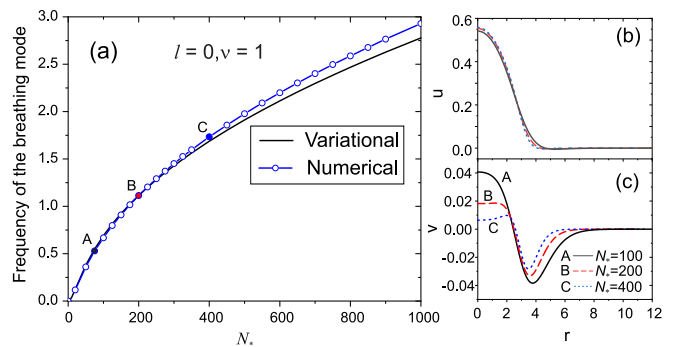


FIG. 4. (a) Breathing compressible mode $\nu = 1$, $l = 0$ frequency, $\omega_{1,0}$, vs N_* obtained numerically (blue line with circles) and in variational approximation (solid black line). Eigenfunctions (b) $u(r)$ and (c) $v(r)$ for three different values of the parameter N_* .

where $R(t)$ and $\beta(t)$ are time-dependent variational parameters. The corresponding Lagrangian is given by

$$\mathcal{L} = -\frac{3}{2} \left[R^2 \dot{\beta} + \frac{1}{2R^2} + 2\beta^2 R^2 \right] + \frac{N_*}{4\sqrt{2}\pi^{3/2}R^3} (1 - R^2). \quad (47)$$

Differentiating Lagrangian (47) one obtains the first Euler-Lagrange equation $\frac{\partial \mathcal{L}}{\partial R} - \frac{d}{dt} \frac{\partial \mathcal{L}}{\partial \dot{R}} = 0$:

$$-3R\dot{\beta} + \frac{3}{2R^3} - 6\beta^2 R - \frac{N_*}{8\pi R^2} \sqrt{\frac{2}{\pi}} + \frac{3N_*}{2(2\pi)^{3/2}R^4} = 0. \quad (48)$$

The second Euler-Lagrange equation reads $\frac{\partial \mathcal{L}}{\partial \beta} - \frac{d}{dt} \frac{\partial \mathcal{L}}{\partial \dot{\beta}} = 0$:

$$\beta = \frac{\dot{R}}{2R}. \quad (49)$$

Substituting Eq. (49) into Eq. (48), we obtain:

$$-\frac{3\ddot{R}}{2} + \frac{3}{2R^3} - \frac{N_*}{8\pi R^2} \sqrt{\frac{2}{\pi}} + \frac{3N_*}{2(2\pi)^{3/2}R^4} = 0. \quad (50)$$

The solution of the last equation in time-independent case is ground state with $\beta = 0$ and $R = R_0$. In the vicinity of stationary solution variational parameter has a form $R(t) = R_0 + \delta(t)$. In the first order, we obtain:

$$\ddot{\delta} + \omega^2 \delta = 0,$$

where

$$\omega^2 = \frac{3}{R_0^4} - \frac{N_0}{6\pi R_0^3} \sqrt{\frac{2}{\pi}} + \frac{4N_0}{(2\pi)^{3/2}R_0^5} = \frac{2}{3N_0} \frac{\partial^2 E}{\partial R^2} \Big|_{R=R_0}, \quad (51)$$

the energy functional is as follows:

$$E = \frac{3}{4R^2} + \frac{N_*}{4\sqrt{2}\pi^{3/2}R^3} (1 - R^2). \quad (52)$$

The stationary state corresponds to the minimum of the energy: $\frac{\partial E}{\partial R} \Big|_{R=R_0} = 0$, where

$$R_0 = \frac{3\sqrt{2\pi^3}}{N_*} \left[1 + \sqrt{1 + \frac{N_*^2}{6\pi^3}} \right]. \quad (53)$$

The breathing mode frequency is given as follows:

$$\omega_b^2 = \frac{2}{3N_*} \frac{\partial^2 E}{\partial R^2} \Big|_{R=R_0}. \quad (54)$$

Figure 4 (a) presents the frequency of the breathing modes. The variational approach (solid black curve) shows good agreement with the numerical solution of the BdG problem (blue curve with circles). Deviations appear only at higher solitonic core masses, corresponding to large N_* , where the local self-interaction dominates over the kinetic energy (TF regime), and the Gaussian-like ansatz (46) becomes less effective in accurately capturing the radial distribution of the BEC core.

Figure 4 (b) and (c) illustrates the eigenfunctions $u(r)$ and $v(r)$ of the breathing mode. For small values of the normalized solitonic mass, N_* , the radial profile of the function $v(r)$, which has a node, exhibits a maximum at the soliton's center. However, as N_* increases, the radial profile becomes deformed, and a local minimum appears in the central region of the soliton. This transformation in the spatial distribution of the perturbation is caused by the repulsive self-interaction. As a result, the density perturbation of a massive solitonic core becomes localized at the surface of the core and does not produce significant density perturbations in the condensate near the peak density region.

VI. SUMMARY AND CONCLUSIONS

We investigated the oscillations of solitonic structures in bosonic ultralight dark matter within the central regions of galaxies. The Bogoliubov-de Gennes (BdG) equations for these perturbations were derived, incorporating both gravitational potential fluctuations and local repulsive interparticle interactions. To solve the integro-differential eigenvalue BdG problem, we developed a numerical method utilizing an orthonormal basis which accounts for the properties of the self-induced gravitational potential. Our numerical solutions provide a comprehensive analysis of the stability and dynamic behavior of solitonic BEC cores, including highly excited states.

We demonstrated that the solitonic core, formed by the balance of gravitational attraction, quantum pressure, and repulsive bosonic interactions, exhibits oscillatory behavior that can significantly influence the central density profiles of dark matter halos. This oscillatory behavior is characterized by specific eigenmodes, whose properties we have analyzed in detail. Using a comprehensive approach that rigorously accounts for both local and nonlocal interactions, we demonstrated that gravitational potential perturbations play an important role

in the dynamics of the solitonic core. The numerical solutions of the BdG problem reveal that these perturbations can lead to breathing modes and other collective excitations, which are consistent with recent theoretical studies. The comparison between our numerical results and variational approaches for the breathing mode frequencies shows good agreement, validating our numerical methods and providing deeper insights into the dynamics of self-gravitating BECs.

These results provide valuable insights for modeling the complex dynamics of ultralight bosonic dark matter and its role in galactic structure formation and evolution. Future work should investigate the effects of these oscillations on observable astrophysical phenomena, including star cluster perturbations and the stability of galactic cores. Furthermore, the results of the BdG analysis can be used for a quantitative study of the thermodynamic properties of ULDM, including the critical temperature for a phase transition in a localized self-gravitating BEC core [38, 39]. Also, condensate depletion – a phenomenon well-established in atomic BEC systems with contact and nonlocal dipole-dipole interactions [40] – can now be accurately addressed using the results obtained here for soliton core excitations. However, simple qualitative estimates for typical BEC solitonic core parameters indicate an exceedingly small contribution from the noncondensed fraction of ultralight bosonic particles. This conclusion arises from the gas parameter $na_s^3 \ll 1$ for realistic values of the s -wave scattering length a_s , implying, as demonstrated previously for atomic BECs [41], a negligible contribution from the anomalous non-condensed fraction at zero temperature. A quantitative analysis of the critical temperature and quantum depletion in self-gravitating localized ULDM structures merits further investigation and will be addressed in future work.

ACKNOWLEDGEMENTS

The authors are partially supported by “Iniziativa Specifica Quantum” of INFN and by the Project “Frontiere Quantistiche” (Dipartimenti di Eccellenza) of the Italian Ministry for Universities and Research. LS is partially supported by funds of the European Union - Next Generation EU: European Quantum Flagship Project “PASQuanS2”, National Center for HPC, Big Data and Quantum Computing [Spoke 10: Quantum Computing], PRIN Project “Quantum Atomic Mixtures: Droplets, Topological Structures, and Vortices”. AY is supported by the BIRD Project ‘Ultracold atoms in curved geometries’, ‘Theoretical analysis of quantum atomic mixtures’ of the University of Padova.

VII. APPENDIX

A. A basis of the hydrogen-like atom

As was pointed out the wave function $\psi_0(r)$ of the fundamental soliton is localized and its profile is well-described in TF approximation for large values of N_* so that for $r \gg r_{TF}$ $\psi_0 \rightarrow 0$ and the gravitation potential tends to Coulomb asymptotic so that trapping potential in Eq. (34) is defined as follows: $\Phi_B(r) = -Z/r$ with $Z = N_*/(4\pi)$. Thus the natural choice of basis functions is the set of the radial wave functions of the hydrogen-like atom (H-like basis):

$$R_{\nu l}(r) = C_{\nu l} e^{-\rho/2} \rho^l L_{\nu}^{(2l+1)}(\rho), \quad (55)$$

and normalization constant, $C_{\nu l}$, is found from the normalization condition (33):

$$C_{\nu l} = \sqrt{\frac{4Z^3 \nu!}{(\nu+l+1)^4 (\nu+2l+1)!}} \quad (56)$$

where $\rho = \frac{2Zr}{\nu+l+1}$. Here $L_{\nu}^{(2l+1)}(\rho)$ is a generalized Laguerre polynomial of degree ν , which defines the number of nodes of the radial profile.

We adopt the hydrogen-like atom basis (H-like basis), utilizing eigenfunctions of the Schrödinger equation for a Coulomb potential with nuclear charge Z to model the gravitational potential in the solitonic core.

As known, the radial wave function of the hydrogen-like atom, $R_{\nu l}(r)$, satisfies the following ordinary differential equation:

$$-\frac{1}{2} \Delta_r^{(l)} R_{\nu l}(r) - \frac{Z}{r} R_{\nu l}(r) = E_{\nu l} R_{\nu l}(r) \quad (57)$$

where the energy $E_{\nu l}$ depends on the main quantum number $\nu+l+1$ as given by Eq. (45).

We note that the eigenfrequencies are well approximated by $\omega_{\nu l} \approx -\mu + E_{\nu l}$, where $E_{\nu l}$ is the energy of the hydrogenlike system (60).

The hydrogen atom basis gives very accurate description of the higher-order states of the BdG system for $\nu \gg 1$ and $l \gg 1$. However, the singular behaviour of the Coulomb potential leads to slow convergence of the expansion for $\nu = 0$ or $l = 0, 1$.

B. Harmonic oscillator basis

The gravitational potential for the lowest-order states can be well approximated by the parabolic potential. Indeed, in TF approximation for $r \ll R_{TF}$ the potential $\Phi_{TF}(r) = -\frac{N_*}{4\pi^2} (1 + \frac{1}{2} \sin r) \approx \Phi_{TF}(0) + \frac{1}{2} \Omega^2 r^2$, where $\Phi_{TF}(0) = -\frac{N_*}{2\pi^2}$, $\Omega^2 = N_*/(12\pi^2)$. Thus, the trapping potential in Eq. (34) can be taken as follows: $\Phi_B(r) = \frac{1}{2} \Omega^2 r^2$. The basis of 3D spherically-symmetric oscillator functions:

$$R_{\nu l}(r) = C_{\nu l} e^{-\rho^2/2} \rho^l L_{\nu}^{(l+1/2)}(\rho^2), \quad (58)$$

$$C_{\nu l} = 2^{\nu+l+1} (\Omega^3/\pi)^{1/4} \sqrt{\frac{\nu!(\nu+l)!}{(2\nu+2l+1)!}} \quad (59)$$

where $\rho = \sqrt{\Omega} r$, normalization constant is found from the normalization condition (33). Here $L_{\nu}^{(2l+1)}(\rho)$ is a generalized Laguerre polynomial of degree ν , which defines the number of nodes of the radial profile.

The corresponding potential $\Phi_B(r) = \frac{1}{2} \Omega^2 r^2$ and the energy $E_{\nu l}$ in Eqs. (34), (37), and (38) is as follows:

$$E_{\nu l} = \Omega \left(2\nu + l + \frac{3}{2} \right). \quad (60)$$

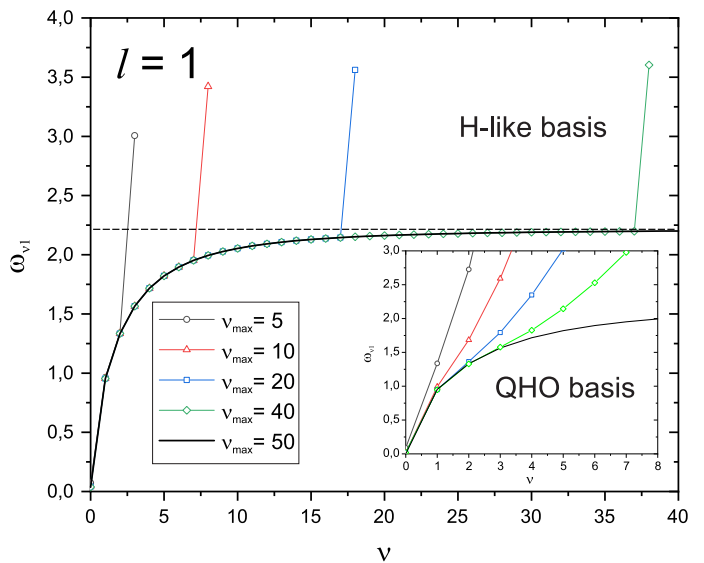


FIG. 5. Illustration of convergence of the eigenvalues $\omega_{\nu l=1}$ for different numbers of the basis functions ν_{\max} using a hydrogen-like atom (H-like) basis. The inset demonstrates the convergence using a quantum harmonic oscillator (QHO) basis, highlighting the faster convergence rate of the hydrogen atom basis.

C. Basis comparison and convergence analysis

As discussed in the main text, obtaining a numerical solution to the BdG problem requires computing the coefficients in the expansion (32), where ν_{\max} is chosen to ensure the desired accuracy in the convergence of the sum (32). We have tested the convergence properties and the optimal selection of the number of basis functions for both the harmonic oscillator and hydrogen-like atom bases.

Figure 5 presents our findings for the mode $l = 1$. The solid curve shows the numerically determined eigenfrequencies of the modes with ν nodes in the radial profile of $\nu_{\max} = 50$ in (32), using the basis of hydrogen-like atoms. The colored open symbols correspond to the

eigenfrequencies obtained with restricted bases for various values of ν_{\max} . The inset displays the same results for the harmonic oscillator basis.

A similar analysis was carried out for different values of the quantum number l , which gives a similar result for

convergence. As shown in Fig. 5, both bases converge to the same eigenvalues $\omega_{\nu l}$. However, the hydrogen-like atom basis exhibits significantly faster convergence, requiring fewer terms in the expansion (32) to accurately reproduce the spectrum.

-
- [1] P.-H. Chavanis, Self-gravitating Bose-Einstein condensates, in *Quantum aspects of Black holes* (Springer, 2014) pp. 151–194.
- [2] E. G. Ferreira, Ultra-light dark matter, *The Astronomy and Astrophysics Review* **29**, 1 (2021).
- [3] M. Baldeschi, G. Gelmini, and R. Ruffini, On massive fermions and bosons in galactic halos, *Physics Letters B* **122**, 221 (1983).
- [4] D. F. Jackson Kimball and K. Van Bibber, *The search for ultralight bosonic dark matter* (Springer Nature, 2023).
- [5] P.-H. Chavanis, Jeans mass-radius relation of self-gravitating Bose-Einstein condensates and typical parameters of the dark matter particle, *Phys. Rev. D* **103**, 123551 (2021).
- [6] J. Veltmaat, J. C. Niemeyer, and B. Schwabe, Formation and structure of ultralight bosonic dark matter halos, *Phys. Rev. D* **98**, 043509 (2018).
- [7] D. J. E. Marsh and J. C. Niemeyer, Strong constraints on fuzzy dark matter from ultrafaint dwarf galaxy Eridanus II, *Phys. Rev. Lett.* **123**, 051103 (2019).
- [8] B. T. Chiang, H.-Y. Schive, and T. Chiueh, Soliton oscillations and revised constraints from eridanus ii of fuzzy dark matter, *Phys. Rev. D* **103**, 103019 (2021).
- [9] H.-Y. Schive, T. Chiueh, and T. Broadhurst, Soliton random walk and the cluster-stripping problem in ultralight dark matter, *Phys. Rev. Lett.* **124**, 201301 (2020).
- [10] X. Li, L. Hui, and T. D. Yavetz, Oscillations and random walk of the soliton core in a fuzzy dark matter halo, *Phys. Rev. D* **103**, 023508 (2021).
- [11] T. D. Yavetz, X. Li, and L. Hui, Construction of wave dark matter halos: Numerical algorithm and analytical constraints, *Phys. Rev. D* **105**, 023512 (2022).
- [12] J. L. Zagorac, I. Sands, N. Padmanabhan, and R. Easter, Schrödinger-Poisson solitons: Perturbation theory, *Phys. Rev. D* **105**, 103506 (2022).
- [13] R. Galazo García, P. Brax, and P. Valageas, Solitons and halos for self-interacting scalar dark matter, *Phys. Rev. D* **109**, 043516 (2024).
- [14] S.-C. Lin, H.-Y. Schive, S.-K. Wong, and T. Chiueh, Self-consistent construction of virialized wave dark matter halos, *Phys. Rev. D* **97**, 103523 (2018).
- [15] D. H. Bernstein, E. Giladi, and K. R. Jones, Eigenstates of the gravitational Schrödinger equation, *Modern Physics Letters A* **13**, 2327 (1998).
- [16] P. Tod and I. M. Moroz, An analytical approach to the Schrödinger-Newton equations, *Nonlinearity* **12**, 201 (1999).
- [17] D. D. Chowdhury, F. C. Van den Bosch, V. H. Robles, P. van Dokkum, H.-Y. Schive, T. Chiueh, and T. Broadhurst, On the random motion of nuclear objects in a fuzzy dark matter halo, *The Astrophysical Journal* **916**, 27 (2021).
- [18] M. Indjin, I.-K. Liu, N. P. Proukakis, and G. Rigopoulos, Virialized profiles and oscillations of self-interacting fuzzy dark matter solitons, *Phys. Rev. D* **109**, 103518 (2024).
- [19] N. P. Proukakis, G. Rigopoulos, and A. Soto, Hybrid model of condensate and particle dark matter: Linear perturbations in the hydrodynamic limit, *Phys. Rev. D* **110**, 023504 (2024).
- [20] K. Asakawa, H. Ishihara, and M. Tsubota, Collective excitations of self-gravitating Bose-Einstein condensates: Breathing mode and appearance of anisotropy under self-gravity, *Progress of Theoretical and Experimental Physics*, ptae078 (2024).
- [21] I.-K. Liu, N. P. Proukakis, and G. Rigopoulos, Coherent and incoherent structures in fuzzy dark matter haloes, *Monthly Notices of the Royal Astronomical Society* **521**, 3625 (2023).
- [22] N. Glennon and C. Prescod-Weinstein, Modifying puyultralight to model scalar dark matter with self-interactions, *Phys. Rev. D* **104**, 083532 (2021).
- [23] R. Harrison, I. Moroz, and K. Tod, A numerical study of the Schrödinger-Newton equations, *Nonlinearity* **16**, 101 (2002).
- [24] K. Schroven, M. List, and C. Lämmerzahl, Self-gravitating Bose-Einstein condensates: Excited solutions and stability, in *The Fourteenth Marcel Grossmann Meeting On Recent Developments in Theoretical and Experimental General Relativity, Astrophysics, and Relativistic Field Theories: Proceedings of the MG14 Meeting on General Relativity, University of Rome “La Sapienza”, Italy, 12–18 July 2015* (World Scientific, 2018) pp. 2043–2048.
- [25] P.-H. Chavanis, Mass-radius relation of newtonian self-gravitating Bose-Einstein condensates with short-range interactions. I. Analytical results, *Phys. Rev. D* **84**, 043531 (2011).
- [26] Y. O. Nikolaieva, A. O. Olashyn, Y. I. Kuriatnikov, S. I. Vilchynskii, and A. I. Yakimenko, Stable vortex in Bose-Einstein condensate dark matter, *Low Temperature Physics* **47**, 684 (2021).
- [27] Y. O. Nikolaieva, Y. M. Bidasyuk, K. Korshynska, E. V. Gorbar, J. Jia, and A. I. Yakimenko, Stable vortex structures in colliding self-gravitating Bose-Einstein condensates, *Phys. Rev. D* **108**, 023503 (2023).
- [28] K. Korshynska, O. O. Prykhodko, E. V. Gorbar, J. Jia, and A. I. Yakimenko, Vortex lines in ultralight bosonic dark matter around rotating supermassive black holes, *Phys. Rev. D* **111**, 023006 (2025).
- [29] J. Sakstein and I. D. Saltas, Dark matter induced stellar oscillations, *Monthly Notices of the Royal Astronomical Society: Letters* **527**, L14 (2024).
- [30] F. S. Guzmán and L. A. Ureña López, Gravitational atoms: General framework for the construction of multistate axially symmetric solutions of the Schrödinger-Poisson system, *Phys. Rev. D* **101**, 081302 (2020).
- [31] T. Matos and L. Arturo Ureña López, Further analysis of a cosmological model with quintessence and scalar dark

- matter, *Phys. Rev. D* **63**, 063506 (2001).
- [32] V. Sahni and L. Wang, New cosmological model of quintessence and dark matter, *Phys. Rev. D* **62**, 103517 (2000).
- [33] H.-Y. Schive, T. Chiueh, and T. Broadhurst, Cosmic structure as the quantum interference of a coherent dark wave, *Nature Physics* **10**, 496 (2014).
- [34] V. Iršič, M. Viel, M. G. Haehnelt, J. S. Bolton, and G. D. Becker, First constraints on fuzzy dark matter from Lyman- α forest data and hydrodynamical simulations, *Phys. Rev. Lett.* **119**, 031302 (2017).
- [35] A. I. Yakimenko, Y. A. Zaliznyak, and Y. Kivshar, Stable vortex solitons in nonlocal self-focusing nonlinear media, *Phys. Rev. E* **71**, 065603 (2005).
- [36] E. Chávez Nambo, A. Diez-Tejedor, A. A. Roque, and O. Sarbach, Linear stability of nonrelativistic self-interacting boson stars, *Phys. Rev. D* **109**, 104011 (2024).
- [37] B. A. Malomed, Soliton models: Traditional and novel, one- and multidimensional, *Low Temperature Physics* **48**, 856 (2022).
- [38] D. A. W. Hutchinson, E. Zaremba, and A. Griffin, Finite temperature excitations of a trapped Bose gas, *Phys. Rev. Lett.* **78**, 1842 (1997).
- [39] S. Giorgini, L. Pitaevskii, and S. Stringari, Thermodynamics of a trapped Bose-condensed gas, *Journal of Low Temperature Physics* **109**, 309 (1997).
- [40] A. R. P. Lima and A. Pelster, Beyond mean-field low-lying excitations of dipolar Bose gases, *Phys. Rev. A* **86**, 063609 (2012).
- [41] M. Rossi and L. Salasnich, Path-integral ground state and superfluid hydrodynamics of a bosonic gas of hard spheres, *Phys. Rev. A* **88**, 053617 (2013).